Sensitivity Analysis and Key Control Factors of Dynamic Compaction Vibration in Miscellaneous Fill Sites

Jianmin Zhu [1*], Baozhi Dong [2], Yukun Wen [2], Yi Liang[3]

[1]School of Civil Engineering, Xi'an University of Architecture and Technology, Xi'an, 710055, China
[2]Shanxi Jin Baodao Foundation Engineering Co., Ltd., Taiyuan 030031, China
[3]China United Northwest Institue for Engineering Design & Research Co., Ltd., Xi'an 710077, China

*zjm1995triumph@163.com

Abstract. To examine the key factors influencing vibration reduction in dynamic compaction, the influence of vibration source distance, hammer height, tamping settlement, and falling distance at energy levels of 4000 kN·m, 12000 kN·m, and 25000 kN·m on a miscellaneous fill site was analyzed. Using the LIBSVM algorithm for modeling and Sobol sensitivity analysis, findings indicate that the primary vibration frequency centers around 15 Hz. Frequency fluctuation increases with tamping energy, but the main frequency remains largely stable. Vibration velocity decreases exponentially with distance from the vibration source, showing three attenuation zones: main (0–30 m), middle (30–60 m), and final (>60 m). Vibration velocity rises initially with hammer height, stabilizing optimally at 0.7 m, then declines in a negative exponential trend. Over cumulative tamping settlement, velocity follows three stages—rapid increase, gradual increase, and stabilization—due to factors like soil compactness, pit depth, and particle rearrangement. Characteristic vibration velocity peaks around an 18 m drop distance, then gradually diminishes. Sensitivity ranking indicates that hammer height and drop distance are the most significant factors, followed by vibration source distance and tamping settlement. Thus, in dynamic compaction design, controlling hammer height and drop distance optimally reduces vibration, while adjusting source distance and tamping settlement offers additional control.

Keywords: Miscellaneous fill; Dynamic compaction; Vibration velocity; Sensitivity analysis

1 Introduction

Dynamic compaction method is a kind of foundation treatment method which can improve foundation strength, increase soil compactness and eliminate collapsibility in a short time. It has the advantages of wide application range, good reinforcement effect and simple construction conditions [1]. However, the dynamic compaction construction process is often accompanied by huge energy and strong vibration waves, which have a

G. Zhao et al. (eds.), *Proceedings of the 2024 6th International Conference on Civil Architecture and Urban Engineering (ICCAUE 2024)*, Advances in Engineering Research 262,
https://doi.org/10.2991/978-94-6463-688-8_26

non-negligible impact on construction personnel, residents and surrounding buildings [1-2].

Research on dynamic compaction vibration domestically and internationally has concentrated on three areas: vibration prevention, isolation, and control. In vibration prevention, Chun et al. [3] and Liu et al. [4] investigated the effects of dynamic compaction on fill foundations and marine cut-off walls, identifying vibration attenuation patterns through experiments and monitoring and providing recommendations for construction and reinforcement. For vibration reduction, Li et al. [5], Chun et al. [3], Wang et al. [6] studied the effectiveness of vibration reduction ditches through simulations and field tests, offering practical insights for engineering applications. In vibration control, numerous field tests have been conducted on soils such as sand [7], sand soil [8], andesite [9], gravel soil [10] compacted at energy levels up to 15000 kN·m. These studies, including those by Wu et al. [11], show a power or exponential relationship between vibration velocity and source distance, contributing valuable data for design. Additionally, Vlček et al. [12], using measured data from gravel soil sites (130-240 kN·m), observed that beyond a soil's original shear strength, the vibration velocity growth rate decreases and terrain elevation amplifies acceleration time histories. Cao et al. [13] explored how factors like tamping energy, drop distance, and hammer diameter affect vibration propagation, adding to the understanding of vibration dynamics. In summary, current research on dynamic compaction vibration control, both domestically and internationally, primarily relies on model tests and numerical simulations. Studies based on actual measurements of high-energy compaction in heterogeneous soil sites are limited. Dynamic compaction vibration is influenced by multiple interacting factors, making it challenging to control through any single factor alone.

This paper examines the field vibration response of a miscellaneous fill site, analyzing how vibration source distance, hammer height, cumulative tamping settlement, and falling distance affect vibration velocity at energy levels of 25000 kN·m, 12000 kN·m, and 4000 kN·m. A comparative test was conducted on the slope top to study the propagation patterns of dynamic compaction vibration across the surface. The findings aim to offer guidance for controlling dynamic compaction vibration in miscellaneous fill engineering projects.

2 Overview of Dynamic Compaction Vibration Test

2.1 Overview of the Test Site

The site is located in the suburbs of Yangquan City, Shanxi Province. The latitude and longitude are 113 ° 34 ' 35.0'E, 37 ° 58 ' 39.9'N. It is a 500 MWh ~ 1000 MWh electrochemical energy storage power station of a power plant. The site is flat as a whole. According to the exploration, the strata are miscellaneous fill (Q_4^{ml}) and sandy shale (C) from top to bottom, and no groundwater is found in the exploration. The basic physical and mechanical properties of the rock and soil are shown in Table1.

Table 1. Physical and mechanical properties of rock and soil index

Index	Sandy shale	Miscellaneous fill
γ/(kN/m^3)	/	18.5
Number of dynamic penetrations$N_{63.5}$	/	7.4
Single axis compressive strength (MPa)	13.42	0.07
RQD	20～30	/
Rock quality grade	IV	/
Modulus of deformation E_0 (MPa)	50	/
Bearing capacity f_a (kPa)	600	/

2.2 Test Equipment

The dynamic compaction vibration test equipment is shown in Fig.1, which mainly includes dynamic compaction machine, three-way vibration velocity sensor, vibrometer and computer app. The nonlinear accuracy of the three-way vibration velocity sensor is 0.2 %, and the ambient temperature is-40 ~ 70 °C. The sensor can be firmly connected with the measured object before testing the acceleration signal without knowing the direction of motion at a certain point. The model of vibrometer is TC-4850-3N, the reading accuracy is 0.1mm / s, and the range is ± 35mm/s. In the dynamic compaction vibration test, the vibration is first manufactured by the dynamic compaction machinery, and the three-way vibration velocity sensor is connected to the vibrometer by the data line to collect the vibration signal. After the test, the test data is exported by the computer app.

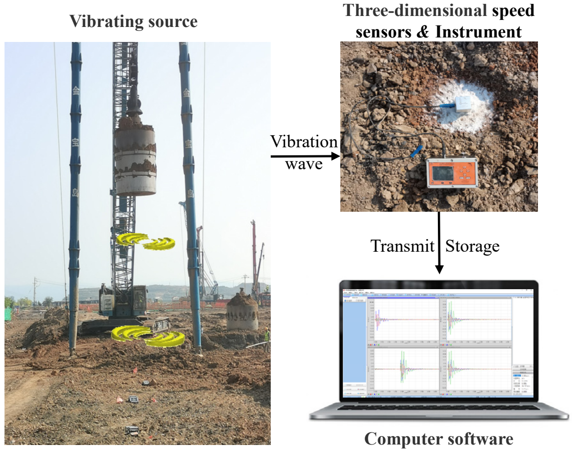

Fig. 1. Dynamic compaction vibration test equipment

2.3 Test Scheme

Based on site geological conditions and reinforcement depth, the following tamping energy levels are established: 4000 kN·m is Suitable for shallow preliminary compaction of loose miscellaneous fill. 12000 kN·m is Suitable for medium thickness miscellaneous fill and shallow sandy shale to enhance bearing capacity. 25000 kN·m is Suitable for reinforcing thick miscellaneous fill and broken sandy shale for deeper effects. Each tamping energy is associated with a measuring line spaced 10 m apart, with 8 measuring points on each line. The vibration source distances are 10 m, 20 m, 30 m, 40 m, 60 m, 80 m, 90 m, and 100 m. The distribution of tamping and check points is shown in Fig. 2, and the parameters for the dynamic compaction vibration test are detailed in Table 2.

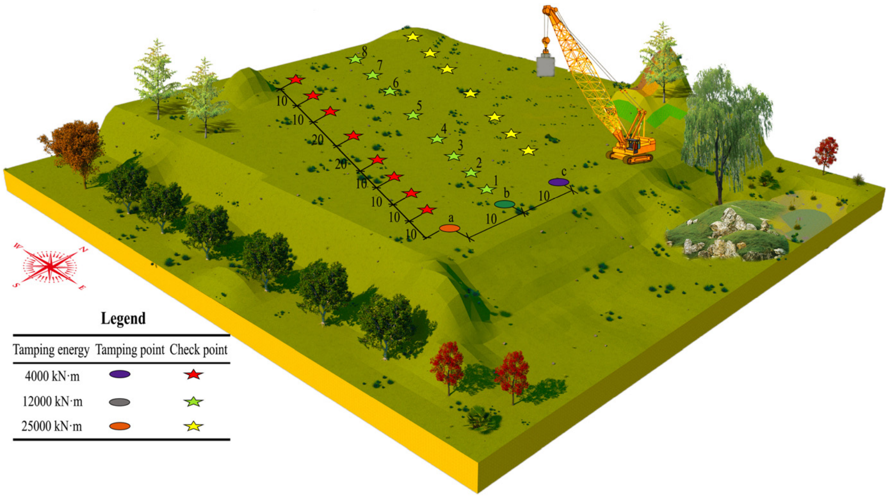

Fig. 2. Distribution of tamping points and check points

Table 2. Dynamic compaction vibration test parameters

Tamping energy / kN·m	Tamping point number	Check point number	Hammer			Height of drop/ m
			Height /m	Diameter / m	Weight/ t	
25000	a	a-(1~8)	3.9		138	18.5
12000	b	b-(1~8)	1.9	2.4	67	18.2
4000	c	c-(1~8)	0.7		25	16.3

3 Test Results and Analysis

3.1 Effect of Tamping Energy on Vibration Frequency Distribution

The distribution of vibration frequency under different tamping energy is shown in Fig. 3.

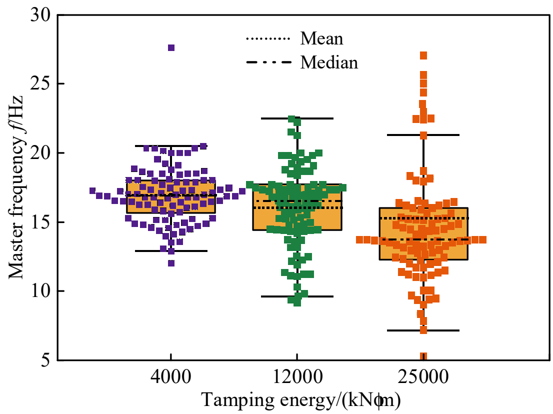

Fig. 3. Vibration frequency distribution

When the tamping energy is 4000 kN·m, 12000 kN·m and 25000 kN·m, the vibration frequency is concentrated in 15 ~ 18 Hz, 14 ~ 17 Hz and 12 ~ 20 Hz respectively, and the median is 16 Hz, 15 Hz and 15 Hz respectively. With the increase of tamping energy, the fluctuation range of vibration frequency gradually expands, but the main frequency distribution is still concentrated at about 15 Hz, indicating that the dynamic compaction energy mainly affects the dispersion and fluctuation of vibration frequency, but has little effect on the main frequency.

3.2 Effect of Vibration Source Distance on Vibration Velocity

The maximum vibration velocity attenuation curve is shown in Fig.4. According to the characteristics of vibration velocity attenuation, the maximum vibration velocity attenuation curve is divided into three stages:

Section I: In the main attenuation section (0–30 m), vibration velocity sharply decreases as energy dissipates. At energy levels of 12000 kN·m and 25000 kN·m, vibration velocity drops by approximately 110 mm/s and 90 mm/s, respectively, and around 40 mm/s at 4000 kN·m, showing that higher energy levels produce significant near-field vibration effects.

Section II: In the middle attenuation section (30–60 m), the vibration velocity attenuation rate slows, with the curve flattening due to soil damping and the heterogeneous nature of the fill. Vibration velocity declines to about 6.05 mm/s at 4000 kN·m, 15.69 mm/s at 12000 kN·m, and 11.63 mm/s at 25000 kN·m, indicating stable attenuation.

Section III: Beyond 60 m, in the final attenuation section, vibration velocity stabilizes across all energy levels. At this distance, vibration velocities remain at approximately 6.05 mm/s for 4000 kN·m, 15.69 mm/s for 12000 kN·m, and 11.63 mm/s for 25000 kN·m, indicating minimal long-distance vibration impact.

From Fig.4, it can be seen that the determination coefficient R^2 of the fitting formula of vibration velocity attenuation curve under each energy level is above 0.99, which indicates that the relationship between vibration velocity and vibration source distance conforms to the negative exponential attenuation law of formula (1).

$$v = a \cdot e^{\frac{-S}{t}} + v_0 \tag{1}$$

a—coefficient, is greater than zero; *e*—constant, 2.718; *t*—coefficient; v_0—constant.

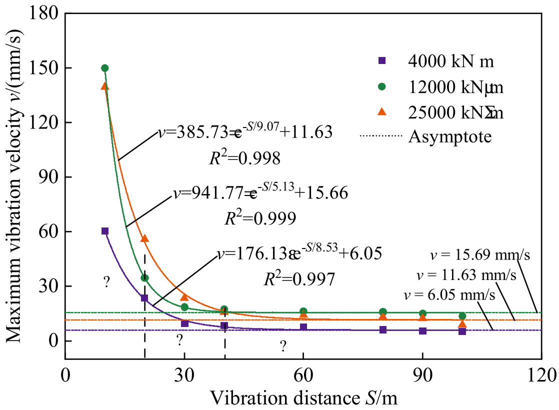

Fig. 4. Maximum vibration velocity attenuation curve

3.3 Effect of Rammer Height on Vibration Velocity

Tamping energy significantly affects dynamic compaction vibration, determined by the drop distance and hammer weight. Given the small variation in drop distances (16.3 m, 18.2 m, and 18.5 m) at energy levels of 4000 kN·m, 12000 kN·m, and 25000 kN·m, the influence of drop distance on vibration velocity is considered negligible. Therefore, only the effect of hammer height is analyzed. As shown in Eq. (2) and Eq. (3), hammer weight is directly proportional to hammer height, allowing a direct assessment of how hammer height impacts vibration velocity.

$$E = m \cdot g \cdot H \tag{2}$$

$$m = V \cdot \rho \tag{3}$$

$$V = \pi \cdot \left(\frac{D}{2}\right)^2 \cdot h \tag{4}$$

Bring the formulas (2) and (3) into (1):

$$E = \pi \cdot \left(\frac{D}{2}\right)^2 \cdot h \cdot \rho \cdot g \cdot H \tag{5}$$

E—tamping energy; *D*—hammer diameter; *h*—hammer height, m; *ρ*—density, iron, approx. 7850 kg/m^3; *g*—gravity, 9.8 m/s^2; *H*—drop, m.

Fig.5 shows the vibration velocity distribution across various hammer heights, with shaded areas representing data density. At hammer heights of 0.7 m, 1.9 m, and 3.9 m, the average vibration velocities are 10.71 mm/s, 25.33 mm/s, and 23.07 mm/s, respectively, with standard deviations of 15.16 mm/s, 39.77 mm/s, and 35.26 mm/s. According to the Mean ± 1SD, vibration velocities fall within 0–25.87 mm/s, 0–65.10 mm/s, and 0–58.33 mm/s for approximately 68% of the data. Overall, the average vibration velocity first increases and then decreases as hammer height rises, concentrating mainly within 0–65.1 mm/s. The data show that vibration stability is highest at 0.7 m, where the standard deviation is lowest.

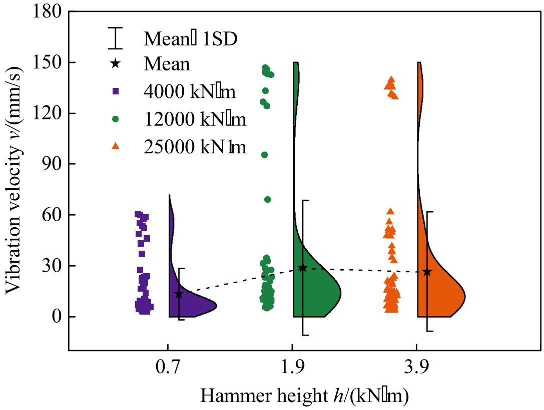

Fig. 5. Vibration velocity distribution

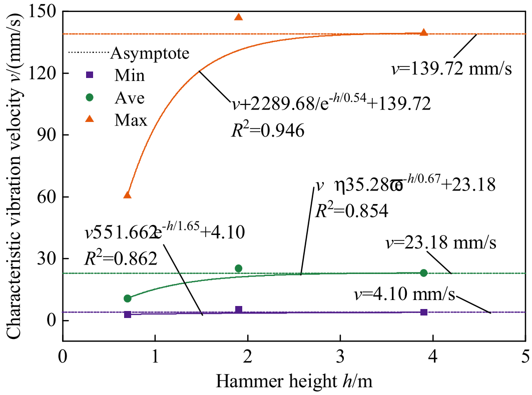

Fig. 6. Relationship between characteristic vibration velocity and hammer height

Fig. 6 shows the maximum, average, and minimum vibration velocities for different hammer heights, illustrating that characteristic vibration velocity initially increases rapidly with height, then stabilizes near asymptotes of 139.72, 23.18, and 4.10 mm/s, following a negative exponential distribution.

$$v = a \cdot e^{\frac{-h}{t}} + v_0 \tag{6}$$

a—coefficient, is less than zero; e—constant, 2.718; t—coefficient; v_0—constant.

Research indicates that hammer height has a limited effect on vibration velocity. While a higher hammer increases impact energy, once it surpasses a certain height, this energy spreads over a broader area, reducing the efficiency of vibration propagation during dynamic compaction. This phenomenon accounts for the rapid initial increase in characteristic vibration velocity followed by stabilization, as well as the decrease in minimum vibration velocity.

3.4 Effect of Ramming Settlement on Vibration Velocity

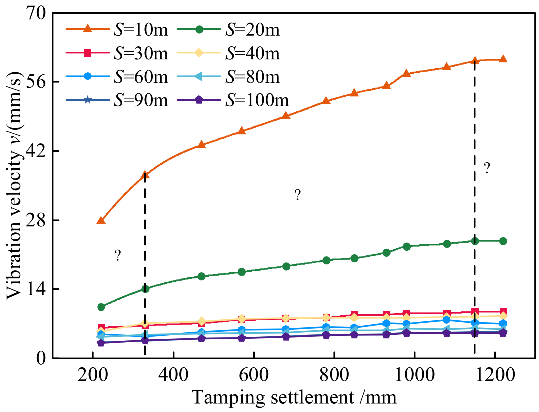

4000 kN·m

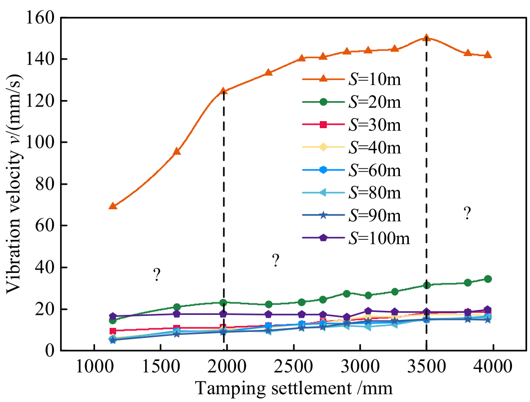

12000 kN·m

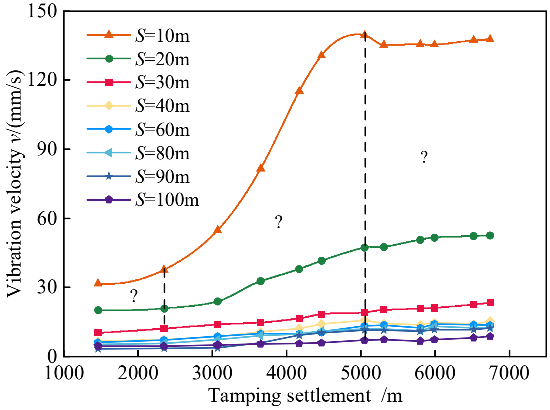

25000 kN·m

Fig. 7. Relationship between vibration velocity and cumulative ramming settlement

Fig. 7 illustrates the relationship between vibration velocity and cumulative tamping settlement, which can be divided into three stages:

Section I (Sudden Increase): Vibration velocity rises rapidly, albeit with a small amplitude. Initially, the soil is loose, and tamping energy primarily facilitates pore compression and particle rearrangement. Consequently, tamping settlement decreases quickly, and the soil's capacity to absorb the impact from the hammer diminishes.

Section II (Slow Increase): Vibration velocity increases more gradually. As cumulative settlement rises, soil compactness improves, reducing its ability to absorb impact energy, leading to a slower increase in vibration velocity [14-15]. At 25000 kN·m, the greater rammer height and wider energy propagation compensate for the attenuation caused by increased ramming pit depth, resulting in a different sequence of stages compared to 4000 kN·m and 12000 kN·m.

Section III (Stabilization): Vibration velocity stabilizes. After multiple tampings, soil density increases, weakening its ability to absorb impact energy. Simultaneously, more energy is transmitted to deeper layers, resulting in low and stable surface vibration velocity.

3.5 Effect of Drop Distance on Vibration Velocity

Fig. 8 illustrates the relationship between vibration velocity and falling distance. Initially, as falling distance increases, characteristic vibration velocity (including maximum, average, and minimum) rises rapidly, peaking at around 18 m before gradually decreasing. This trend indicates that while increased drop distance elevates tamping energy and consequently ground vibration velocity, it also leads to greater tamping settlement. This increased settlement allows vibration energy to penetrate deeper, reducing energy density. As a result, the vibration velocity measured at the ground surface diminishes with greater fall distance.

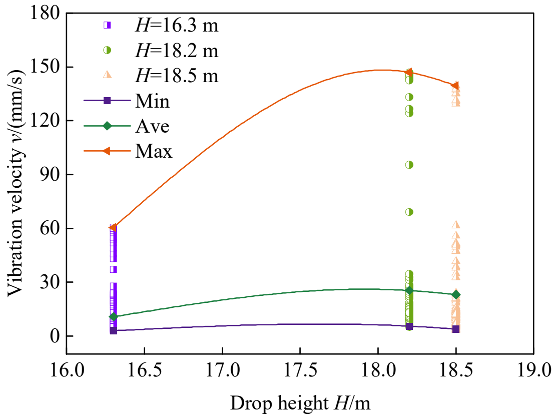

Fig. 8. Relationship between vibration velocity and falling distance

4 Sensitivity Analysis of Influence Factors of Dynamic Compaction Vibration

Support Vector Machine (SVM) is a machine learning method developed by Vapnik et al. [16] that is based on the principle of structural risk minimization in statistical theory. It represents an advanced version of neural network algorithms, effectively addressing their limitations, such as network structure determination, overfitting, underfitting, and local minima. SVM excels in small sample sizes and nonlinear regression problems. The LIBSVM algorithm enhances SVM by incorporating the strengths of the Sequential Minimal Optimization algorithm, enabling precise representation of high-dimensional functions [17].

To establish a model between the influencing factors of dynamic compaction vibration and the vibration velocity with good adaptability, the following assumptions are made:

(1) The input variables are independent of each other, and there is no obvious correlation.

(2) The output of the LISVM model is smooth and measurable when the input variable changes, ensuring that the variance is decomposable.

(3) The kernel function can properly map the input data to capture the nonlinear relationship, and the mapping will not make the relationship between variables too complex.

(4) Variance decomposition can quantify the contribution of each input variable.

A total of 288 sets of dynamic compaction vibration test data were obtained in this test, which were brought into the model as training samples. Suppose that the input sample x and the vibration velocity v obey the function $v=f(x)$. Firstly, the data set is fitted with the function $g(x)=\omega\Phi(x)+b$ and the function $R=|f(x)-g(x)|$ is minimized. According to the principle of structural risk minimization, $g(x)$ should minimize J:

$$J = \frac{1}{2} \| \omega \|^2 + c \sum_{i=1}^{k} L\left(g(x_i), y_i\right) \tag{7}$$

That is:

$$\min J \tag{8}$$

$$\text{s.t.} \begin{cases} y_i - (\omega \cdot x) - b \leqslant \varepsilon + \xi_i \\ (\omega \cdot x) + b - y_i \leqslant \varepsilon + \xi_i^* \\ \xi_i, \xi_i^* \geqslant 0 \end{cases} \tag{9}$$

ω-weight vector; b-deviation; $\varepsilon > 0$, fitting accuracy; ξ_i, ξ_i^* is the error variable, indicating the part above and below the target value exceeding ε, $i = 1, 2, \cdots, k$; c is the regularization parameter. The Lagrange optimization method is used to transform the above problem into a dual problem:

$$\begin{aligned} &\max[-\frac{1}{2}\sum_{i,j=1}^{k}(\alpha_i - \alpha_i^*)(\alpha_j - \alpha_j^*)(x_i \cdot x_j) - \\ &\varepsilon \sum_{i=1}^{k}(\alpha_i + \alpha_i^*) + \sum_{i=1}^{k} y_i(\alpha_i^* - \alpha_i)] \end{aligned} \tag{10}$$

$$\text{s.t.} \begin{cases} \sum_{i=1}^{k}(\alpha_i - \alpha_i^*) = 0 \\ \alpha_i, \alpha_i^* \in [0, c] \end{cases} \tag{11}$$

$\alpha_i - \alpha_i^*$ is the Lagrange factor, greater than 0.

The kernel function $K(x_i \cdot x_j)$ is used to replace the above two-dimensional linear problem into a high-dimensional nonlinear problem, and the regression function can be obtained by solving:

$$f(x) = (\omega \cdot x) + b = \sum_{i=1}^{k}(\alpha_i^* - \alpha_i) K(x_i \cdot x_j) + b \tag{12}$$

To quantify the influence of various factors on the dynamic compaction vibration, the functional relationship between the vibration velocity and the vibration source distance S, the hammer height h, the ramming amount D, and the drop distance H is expressed as $v = f(x)$. The Sobol sensitivity analysis method is used to analyze the dynamic compaction vibration data, where $x = [S, h, D, H]^T$ is a four-dimensional independent random variable. Firstly, assuming that the expected value of each component is zero and orthogonal to each other, the function can be decomposed into the sum of all components.

$$f(x)=f_0+\sum_{i=1}^{4}f_i(x_i)+\sum_{i_1=1}^{4}\sum_{i_2=i_1+1}^{4}f_i(x_{i_1},x_{i_2})+\cdots+f_{i,\cdots,4}(x_1,x_2,\cdots,x_4) \tag{13}$$

f_0 is the average value of the function.

Using the orthogonality between variables, the total variance of $f(x)$ can be expressed as :

$$D[f(x)]=\int_0^1 f^2(x)\mathrm{d}x-f_0^2 \tag{14}$$

Each variance can be calculated by the following formula:

$$D_{i_1,\cdots,i_z}=\int_0^1 f_{i_1,\cdots,i_z}^2(x_{i_1},\cdots,x_{i_z})\mathrm{d}x_{i_1}\cdots\mathrm{d}x_{i_z} \tag{15}$$

$$1\leqslant i_1<\cdots<i_z\leqslant 4,\quad z=1,2,3,4.$$

The Sobol global sensitivity index (Q) can be obtained by the variance ratio:

$$S_{i_1,i_2,\cdots,i_z}=\frac{D_{i_1,i_2,\cdots,i_z}}{D[f(x)]} \tag{16}$$

When $z=i$, the calculation result is the main effect index (M) of the parameter x_i, which indicates the main influence of the parameter x_i on the output $f(x)$.

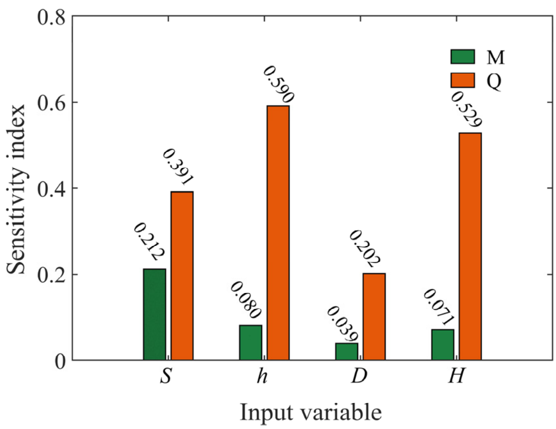

Fig. 9. Sensitivity index

The sensitivity index histogram of vibration source distance *S*, hammer height *h*, ramming settlement *D* and drop distance *H* to vibration velocity *v* is shown in Fig.9. From the figure, the global sensitivity of the above factors to vibration velocity is as follows:

$$h > H > S > D \tag{17}$$

The results indicate that hammer height (*h*) and drop distance (*H*) are the most influential factors affecting vibration velocity, with full effect indices of 0.590 and 0.529, respectively, and main effect indices of 0.080 and 0.071. Vibration velocity is primarily impacted by interactions with other factors. The vibration source distance (*S*) has a full effect index of 0.391 and a main effect index of 0.212, reflecting moderate direct and indirect effects. Tamping settlement (*D*) has the least influence, with a full effect index of 0.202 and a main effect index of 0.039, mainly affecting vibration velocity indirectly through interactions.

Based on the research findings, prior to dynamic compaction construction, the optimal hammer height and drop distance should be established through field tests, followed by the formulation of a corresponding construction plan. In sensitive areas, it is advisable to choose a lower hammer height and drop distance to minimize vibration intensity. Additionally, the vibration source distance should be carefully adjusted to maximize the distance from nearby buildings, reducing the risk of vibration propagation. If adjusting the vibration source distance is not feasible, vibration can be mitigated by altering the hammer height and drop distance. Moreover, a real-time vibration monitoring system should be implemented to enable timely adjustments to construction parameters, preventing excessive vibration. To minimize soil disturbance and ensure project quality and safety, tamping settlement should be controlled, with a reasonable maximum settlement limit set, and compaction should be performed in stages.

5 Conclusions

This paper examines the effects of vibration source distance, hammer height, ramming settlement, and drop distance on vibration velocity at energy levels of 25000 kN·m, 12000 kN·m, and 4000 kN·m on a flat site of miscellaneous fill. The Sobol sensitivity analysis method was employed to rank the influence of these factors on the vibration velocity of dynamic compaction, leading to the following conclusions:

(1) The main frequency of vibration is primarily centered around 15 Hz across different tamping energy levels. Although the range of frequency fluctuations increases with higher tamping energy, the main frequency remains largely unaffected, indicating that tamping energy primarily influences the dispersion and fluctuation of vibration frequency.

(2) The maximum vibration velocity attenuation curve can be divided into three stages: Main Attenuation Section: A sharp decrease in vibration velocity occurs within 0 to 30 m. Middle Attenuation Section: The attenuation rate slows down between 30 and 60 m. End of Attenuation Section: Beyond 60 m, vibration velocity stabilizes. The relationship between vibration velocity and vibration source distance follows a negative exponential attenuation law of $v = a \cdot e^{-S/t} + v_0$.

(3) The vibration velocity increases first and then decreases with the increase of hammer height. Under different hammer heights, the vibration velocity is mainly concentrated in the range of 0 ~ 65.1 mm / s; when the hammer height is 0.7 m, the concentration and stability of the vibration velocity are relatively high, and the characteristic vibration velocity and hammer height show a negative exponential distribution of $v = a \cdot e^{-h/t} + v_0$.

(4) The growth rate of vibration velocity is divided into three stages with the increase of cumulative rammed settlement: sudden increase stage, which reflects the influence of soil compression and particle rearrangement on vibration velocity; the slow increase section reflects that the vibration velocity is affected by the comprehensive effect of soil compactness, tamping pit depth and hammer height, and the propagation energy gradually increases. The stable section reflects that the vibration velocity is affected by the soil compactness and the depth of the tamping pit.

(5) As drop distance increases, characteristic vibration velocity (maximum, average, and minimum) rises rapidly to a peak before gradually decreasing, with the peak occurring at approximately 18 m.

(6) The research findings indicate that the full effect indices for hammer height, drop distance, vibration source distance, and cumulative tamping settlement are 0.590, 0.529, 0.391, and 0.202, respectively. The main effect indices are 0.080, 0.071, 0.212, and 0.039. Hammer height, drop distance, and cumulative tamping settlement primarily affect vibration velocity through interactions with other factors, while vibration source distance has both direct and indirect effects. Therefore, in designing dynamic compaction, it is crucial to control the hammer height and drop distance to optimize vibration velocity, while also reasonably selecting the vibration source distance and ramming settlement to further mitigate dynamic compaction vibrations.

This paper only conducts a sensitivity analysis of the factors influencing dynamic compaction vibration based on test data. In future research, methods such as laboratory model tests, numerical simulation, and theoretical analysis could be used to explain the reasons for the varying impact of different factors on vibration. Moreover, as the findings of this study are based on a miscellaneous fill site, it remains to be verified whether dynamic compaction vibration responses in other soil types conform to the patterns observed in this study.

Acknowledgements

The project presented in this article is supported by National Natural Science Foundation of China (Grant Nos. 42277151, 42307277); Shaanxi Province Qin Chuangyuan "Scientist+Engineer" Team Construction Project (Grant Nos. 2022KXJ-086).

References

1. Liu Hanlong, Zhao Minghua. Research progress of foundation treatmen Review of ground improvement technical and its application in China[J]. China Civil Engineering Journal, 2016, 49 (01): 96-115. DOI: 10.15951/j.tmgcxb.2016.01.012.

2. Sieradzki M P, Engineer S G. Deep dynamic compaction for subgrade improvements within the Port of Long Beach, California[J]. Inżynieria Morska i Geotechnika, 2017 (2): 78-82. https://api.semanticscholar.org/CorpusID:109413681.
3. Chunqing, Pan Jianwu. Damping effect of damping ditch in dynamic compaction construction [J]. Journal of Vibration and Shock, 2010, 29 (06): 115-120 + 239-240. DOI: 10.13465/j.cnki.jvs.2010.06.043.
4. Liu Bo, Li Haibo, Feng Haipeng et al. Impact test and safety monitoring of dynamic compaction construction vibration on offshore cutoff wall [J]. Rock and Soil Mechanics, 2012,33 (10): 3073-3080. DOI: 10.16285/j.rsm.2012.10.046.
5. Li Run, Jian Wenbin, Kang Rongtao. Study on vibration attenuation law of fill foundation reinforced by dynamic compaction [J]. Chinese Journal of Geotechnical Engineering, 2011,33 (S1): 253-257. http://www.cgejournal.com/cn/article/id/14263.
6. Wang G, Yin Y, Wang J. Vibration safety evaluation and vibration isolation control measures for buried oil pipelines under dynamic compaction: A case study[J]. Soil Dynamics and Earthquake Engineering, 2023, 167: 107783. DOI: 10.1016/j.soildyn.2023.107783.
7. Fathi Afshar N, Hamidi A, Tavakoli Mehrjardi G. Impact of diffraction on screening of dynamic compaction waves with barriers[J]. Innovative Infrastructure Solutions, 2024, 9(6): 184. DOI:10.1007/s41062-024-01502-9.
8. Rollins K M, Jorgensen S J, Ross T E. Optimum Moisture Content for Dynamic Compaction of Collapsible Soils[J]. Journal of Geotechnical and Geoenvironmental Engineering, 1998, 124(8): 699-708. DOI:10.1061/(ASCE)1090-0241 (1998)124:8(699).
9. Wu J, Ma L, Shi J, et al. Investigation of ground vibration of full-stone foundation under dynamic compaction[J]. Shock and Vibration, 2019, 2019: 1-11 DOI:10.1155/2019/2631797.
10. Wu S, Wei Y, Zhang Y, et al. Dynamic compaction of a thick soil-stone fill: Dynamic response and strengthening mechanisms[J]. Soil Dynamics and Earthquake Engineering, 2020, 129: 105944. DOI: 10.1016/j.soildyn.2019.105944.
11. Wu B, Ni W, Shi B, et al. Study on Elevation Effect of Vibration Velocity by Dynamic Compaction on Loess High Slope Based on Dimensional Analysis Method[J]. International Journal of Geomechanics, 2024, 24(6): 04024107. DOI: 10.1061/ijgnai.gmeng-9483.
12. Vlček J, Gago F, Mihálik J, et al. Investigation of dynamic effect of rapid impact compaction[J]. Scientific Reports, 2024, 14(1): 21364. DOI: 10.1038/s41598-024-72728-x
13. Cao Li, Bian Haiding, Zhang Zhe, et al. Model test study on vibration attenuation law of high energy dynamic compaction loess foundation[J]. Science Technology and Engineering, 2023, 23(15): 6581-6590. DOI: 10.12404/j.issn. 1671-1815.2023.23.15.06581.
14. Yan Bo, Lin Peiyuan, Yu Haitao, et al. Analysis of settlement and tamping energy dissipation[J]. Chinese Journal of Geotechnical Engineering, 2011 (S1): 4. http://www.cgejournal.com/article/id/14262.
15. Lopes P, Costa P A, Calçada R, et al. Influence of soil stiffness on building vibrations due to railway traffic in tunnels: Numerical study[J]. Computers and Geotechnics, 2014, 61: 277-291. DOI:10.1016/J.COMPGEO.2014.06.005.
16. Vapink V. Statistical learning theory [M]. New York: Wiley, 1998.
17. Aceña V, de Diego I M, Fernández R R, et al. Support subsets estimation for support vector machines retraining[J]. Pattern Recognition, 2023, 134: 109117. DOI: 10.1016/j.patcog.2022.109117.